Pakistan Veterinary Journal

ISSN: 0253-8318 (PRINT), 2074-7764 (ONLINE)
DOI: 10.29261/pakvetj/2026.136

RESEARCH ARTICLE

H3K18 Lactylation Couples hCG-Induced Lactate Accumulation to Progesterone Receptor-Dependent Ovulation

Xiumei Lu[1], Gang Wu[1], Hongmin Li[1], Benlong Hua[1], Xinyi Zhou[1], Junzhuo Deng[1], Honglin Liu[1] and Ming Shen[1*]

[1]College of Animal Science and Technology, Nanjing Agricultural University, Nanjing, 210014, China
*Corresponding author: shenm2015@njau.edu.cn

ARTICLE HISTORY (25-1130)

Received: November 22, 2025
Revised: April 29, 2026
Accepted: May 09, 2026
Published online: June 05, 2026

Key words:
Granulosa cell
HCG
Lactylation
Ovulation
Progesterone receptor

ABSTRACT

Ovarian follicle development occurs within a physiologically hypoxic microenvironment, accompanied by the gradual accumulation of lactate derived from glycolysis. However, its role in the regulation of ovulation remains incompletely understood. In this study, 42 three-week-old female ICR mice were randomly divided into two groups of 21 each: the PMSG group and the PMSG + hCG group, to establish an hCG-induced superovulation mouse model. Samples were collected at 6h, 10h, and 14h after hCG injection, with seven samples per group at each time point. The result indicated the lactate concentration in ovarian granulosa cells (GCs) was significantly increased after hCG stimulation, peaking at 14h post-superovulation, suggesting a potential role for lactate during the ovulatory process. From these results, additional pharmacological interventions were performed in parallel to hCG treatment， such as Oxamate (inhibitor of lactate) group, Oxamate + Lactate group (lactate supplementation) and the C646 group (lactylation inhibition). To further understand how lactate metabolism regulates ovulation, we employed Western blot, qPCR, and ChIP-qPCR to examine its underlying molecular mechanism. We found that hCG-induced lactate accumulation selectively up-regulated histone H3 lysine 18 lactylation (H3K18la) in GCs. It was enriched on the promoter of *Pgr*, enhancing its transcriptional activation. Thus, enhancing PR protein expression and the transcriptional program of downstream ovulation-related genes. Pharmacological inhibition of lactate dehydrogenase or disruption of histone lactylation significantly decreased H3K18la modification and *Pgr* expression, inhibiting the efficacy of hCG-stimulated ovulation. In contrast, the addition of lactate from outside sources only partially rescued these effects. In order to confirm that the regulation is species-conserved, primary porcine granulosa cells were isolated and cultured in vitro, corresponding drug intervention confirmed that hCG promote PR protein lactylation, nuclear translocation, and transcriptional activation of downstream ovulation related genes via lactate accumulation. In conclusion, our results show here that hCG upregulates the H3K18la modification through inducing lactate accumulation which couples the hormonal signal with PR activation and its downstream gene expression to promote ovulation. Histone lactylation might be a new target of intervention in ameliorating human reproductive disorders or enhancing livestock.

To Cite This Article: Lu X, Wu G, Li H, Hua B, Zhou X, Deng J, Liu H and Shen M, 2026. H3K18 lactylation couples hCG-Induced lactate accumulation to progesterone receptor-dependent ovulation. Pak Vet J, 46(6): 1417-1428. http://dx.doi.org/10.29261/pakvetj/2026.136

INTRODUCTION

Ovulation represents a fundamental event in mammalian reproduction, culminating with the extrusion of a mature, fertilizable oocyte as well as the development of the corpus luteum. This process is under tight control via the hypothalamic-pituitary-ovarian axis, where timely pulses of gonadotropins regulate follicle maturation and the transition to ovulation. In particular, the preovulatory surge of luteinizing hormone (LH) and its clinical surrogate human chorionic gonadotropin (hCG) act as the proximate molecular trigger that converts a preovulatory follicle into an ovulatory follicle. Follicular growth and granulosa cell differentiation are supported by an earlier FSH-driven amplification phase that precedes the LH peak (Hunzicker-Dunn and Mayo, 2015). The terminal events leading to

follicle rupture are then executed under the control of multiple local and systemic mediators (Madogwe *et al*., 2021; Cho *et al*., 2024; Johannsen *et al*., 2024; Zeng *et al*., 2024), including EGF-like factors (Conti *et al*., 2006), progesterone (Kim *et al*., 2009), and prostaglandins (Sirois *et al*., 2004), which together coordinate extracellular matrix remodeling, vascular and inflammatory responses; culminating in follicular wall breakdown and capture of the released oocyte by the oviductal fimbria for potential fertilization (Holesh *et al*., 2026).

At the cellular level, the preovulatory LH surge is decoded by granulosa cells through LH receptor engagement and activation of the adenylyl cyclase-cAMP-PKA signaling axis, which rapidly initiates a transient transcriptional program required for steroidogenic shifts, proteolytic remodeling, and other effector activities that culminate in follicle rupture and oocyte release (Breen *et al*., 2013). Because human chorionic gonadotropin (hCG) and luteinizing hormone (LH) are highly homologous, sharing approximately 80–85% sequence identity in the β-subunit and exhibiting antibody cross-reactivity (Stenman and Alfthan, 2013), hCG is commonly used together with pregnant mare serum gonadotropin (PMSG) in experimental, clinical, and livestock settings (Park *et al*., 2015; Kim and Yoon, 2021). This combination mimics the endogenous LH surge and permits precise timing of ovulation for both mechanistic studies and practical reproductive management. Importantly, the fleeting nature of the hormonal input suggests that chromatin-level control and post-translational modifications are required to convert a short endocrine signal into a tightly timed transcriptional program.

The progesterone receptor (PR) is central to the LH/hCG-driven transcriptional response. In mural granulosa cells, PR is rapidly induced by the LH/hCG surge, peaking 4-8h after hCG stimulation in mice (Robker *et al*., 2000); PR-null mice fail to ovulate, and pharmacological PR blockade prevents ovulation across species(Bishop *et al*., 2016; Schütt *et al*., 2018; Park *et al*., 2020; Shynlova *et al*., 2022) PR activates downstream effectors that execute ovulation: *Adamts1* and *Ptgs2* drive extracellular-matrix remodeling and prostaglandin production (Robker *et al*., 2000); *Runx1/Runx2* govern granulosa differentiation (Dinh *et al*., 2023); proteases (e.g., *Ctsl*) and vasoactive factors such as *Edn2* mediate tissue breakdown and vascular responses (Sriraman *et al*., 2008); and *Adam8* is also implicated in follicular remodeling (Choi *et al*., 2011; Migone *et al*., 2016).

In the preovulatory follicle, granulosa cells reside in a relatively ischemic and hypoxic microenvironment and display elevated glycolysis with progressive accumulation of lactate in follicular fluid and cells (Wu *et al*., 2015; Sonigo *et al*., 2019; Lim *et al*., 2021; Tang *et al*., 2021). Apart from being an end product of metabolism, lactate has also emerged as a signaling metabolite that could regulate gene expression in many different biological systems (Certo *et al*., 2022). The recent identification of histone lysine lactylation (Kla) has provided such a link by directly linking the level of lactate inside cells to epigenetic control of transcription (Zhang *et al*., 2019). Of these modifications, histone H3 lysine 18 lactylation (H3K18la) is enriched at promoters and has been linked to transcriptional activation. Studies in macrophages and tumor cells show that H3K18la can promote the expression of specific gene programs related to immune responses and metabolic reprogramming (Zhang *et al*., 2019; Yu *et al*., 2021; Ji *et al*., 2025; Li *et al*., 2025).

Although the regulatory roles of lactate in physiological and pathological processes have been extensively studied and reported, to date, no studies have been published on the role of lactate or lactate-mediated lactylation in follicular ovulation. Our previous research only confirmed that histone lactylation participates in hCG-induced luteinization (Wu *et al*., 2024), while its direct role in ovulation remains unclear. To address this research gap, the present study systematically investigates the regulatory roles of lactate and its lactylation modification in follicular ovulation using a multi-species strategy that combines in vivo mouse experiments with in vitro cellular models from both porcine and human origins. This cross-species approach allows us to evaluate the generalizability and translational potential of our findings across different mammalian species.

MATERIALS AND METHODS

Animals: All animal procedures were performed in accordance with the Guidelines for the Care and Use of Animals in Research and Teaching and approved by the Institutional Animal Care and Use Committee of Nanjing Agricultural University (Nanjing, China), Approval No.: [SYXK (Su) 2022–0031]. Female ICR mice (3-4 weeks old) were purchased from Qing Long Shan Animal Breeding Center (Nanjing, China). This study employed a completely randomised design, with mice in each group weighed prior to the experiment to ensure no baseline differences. Mice were then randomly allocated to experimental groups using a random number method. Mice were housed seven per cage in a temperature-controlled room (22±2℃) under a 12h light/dark cycle, with ad libitum access to standard chow and water. Mice were randomly assigned to five groups（n=7）: (1) PMSG group, (2) PMSG + hCG group, (3) Oxamate group, (4) Oxamate + Lactate group, and (5) C646 group. All mice initially received an intraperitoneal injection of 10IU pregnant mare serum gonadotropin (PMSG； Ningbo Second Hormone Factory) to stimulate follicular development. After 48h, mice in the relevant groups were injected intraperitoneally with 10IU human chorionic gonadotropin (hCG； Ningbo Second Hormone Factory) to induce ovulation. At the time of hCG administration, intervention groups were treated intraperitoneally with either sodium oxamate (S818460, Macklin; 750mg/kg; inhibitor of lactate production), sodium oxamate (750mg/kg) plus sodium lactate (71718-10G, Sigma-Aldrich；550mg/kg; lactate replenishment), or C646 (HY-13823, MedChemExpress；15mg/kg; a histone lactylation inhibitor). The doses of all drugs involved in this study were primarily determined by reference to our laboratory's previously published article (Wu *et al*., 2024). Given that the drug treatment duration in the present study was shorter than that in the reference study, we moderately increased the drug concentrations to achieve comparable pharmacological effects, while remaining within the safety ranges recommended by the manufacturers' instructions.

All adjusted doses were validated by pilot experiments to confirm the absence of overt cytotoxicity or adverse effects in animals. After treatment, mice were euthanized at the designated time points, and ovaries and other relevant tissues were collected for subsequent analyses. To ensure objectivity and unbiased outcome assessment, blinding was implemented for all outcome measures. Specifically, all samples (including Western blot membranes and tissue sections) were recorded by an independent researcher who was not involved in group allocation prior to analysis. The investigators responsible for outcome assessment were completely blinded to group assignment throughout the entire analysis process, and the codes were not broken until all data collection and analysis were completed. In addition, measurements of animal body weight and tissue weight were performed by an investigator unaware of group allocation.

Collection and counting of mouse oocytes: Bilateral oviducts were dissected from euthanized mice and immediately placed into pre-equilibrated droplets of M2 medium (M7167; Sigma-Aldrich) under mineral oil. Under a stereomicroscope, each oviduct was gently held with fine forceps, and a 1mL syringe needle was used to make a small longitudinal incision along the ampulla to release the cumulus–oocyte complexes (COCs). The collected COCs were transferred to fresh M2 medium and mixed with an equal volume of hyaluronidase solution (H3506; Sigma-Aldrich) to remove cumulus cells. The mixture was incubated at 37°C in a 5% CO_2 incubator for approximately 1min until the cumulus cells were completely dispersed. The denuded oocytes were then washed and transferred into a new droplet of M2 medium using a finely drawn glass pipette. The total number of oocytes retrieved from each mouse was counted and recorded under the stereomicroscope. During outcome assessment, samples were coded so that investigators performing oocyte counting were blinded to the group allocation.

Cell culture and treatment: Mice ovaries were bilaterally collected from mice in each experimental group and immediately placed in pre-warmed F-12 medium supplemented with 10% fetal bovine serum (FBS; C11330500BT, Gibco) and 1% penicillin–streptomycin. Under a stereomicroscope, large antral follicles visible on the ovarian surface were carefully punctured using a 1mL syringe needle to release follicular fluid and granulosa cells. The released contents were collected into a centrifuge tube and centrifuged at 1000rpm for 5min. The supernatant was discarded, and the cell pellet was resuspended in pre-warmed phosphate-buffered saline (PBS; SH30256.01, Cytiva) at 37°C and washed once. After a second centrifugation at 1000rpm for 5min, the supernatant was removed, and the resulting pellet was collected as isolated granulosa cells for subsequent analyses. Porcine ovaries were obtained from a local slaughterhouse and thoroughly rinsed with sterile saline. Follicular fluid was aspirated from visible antral follicles using a sterile 10mL syringe and transferred to sterile centrifuge tubes. The samples were centrifuged at 1000rpm for 5min at room temperature. The supernatant was discarded, and the cell pellet containing porcine granulosa cells was resuspended in pre-warmed PBS (37°C) and washed twice. Cells were then seeded in F-12 medium supplemented with 15% FBS and cultured at 37°C in a humidified atmosphere of 5% CO_2 for 36h to allow attachment. After attachment, cells were gently washed twice along the dish walls with pre-warmed PBS (37°C), and the medium was replaced with F-12 containing 10% FBS for continued culture. When cells reached approximately 70% confluence, treatments were initiated. The KGN human ovarian granulosa-like tumor cell line was used as an in vitro human model to complement the findings from porcine and mouse experiments. Although tumor-derived, KGN cells retain key functional characteristics of primary granulosa cells (e.g., steroidogenesis and gonadotropin responsiveness) and are widely used in reproductive biology research (Wu *et al*., 2024), allowing us to assess the translational relevance of our findings to human ovarian physiology. Briefly, the cell line is passaged to approximately 70% confluency and then treated with drug. For pharmacological interventions, cells in the lactate inhibition group were pretreated with 20mM sodium oxamate for 2h, followed by stimulation with either 15IU/mL hCG or 20mM sodium lactate, as specified in the experimental design. Doses were determined by reference to our previous study (Wu *et al*., 2024) with a moderate increase, validated by pilot experiments.

Determination of intracellular lactate content: In each experimental group, granulosa cells were collected from the ovarian follicles of three randomly selected mice and pooled into one tube to constitute a single biological sample for lactate content measurement. A total of 12 mice per group were used, yielding 4 pooled samples (n=4 per group, where n represents the number of pooled samples). This pooling strategy was necessary due to the limited yield of granulosa cells from a single mouse ovary. All statistical analyses were performed using these pooled samples as the independent statistical unit. The cells were lysed in ice-cold cell lysis buffer (Beyotime), and phenylmethylsulfonyl fluoride (PMSF) was added as a protease inhibitor. Incubated at ice for 30min, the lysates were centrifuged at 12,000×g for 15min at 4°C, and the supernatants obtained were kept for further analysis. The intracellular lactate content was measured by a Lactic Acid Assay Kit (A019-2-1, Nanjing Jiancheng Bioengineering Institute) according to the instruction manual. The lactate level was normalized with respect to total protein content, which was determined by bicinchoninic acid (BCA) assay. The final lactate value was calculated according to the standard curve.

Western blots: To obtain sufficient protein for western blotting, granulosa cells from four randomly selected mice were pooled to form a single assay sample. Per group, cells from 12 mice were used to prepare three such pooled samples (n=3). These pooled samples served as independent statistical units for all analyses. The granulosa cells were lysed in ice-cold cell lysis buffer (Beyotime) containing the protease inhibitor PMSF. This pooling strategy was necessary because the protein yield from a single mouse ovary was insufficient for reliable western blot detection. The lysates were centrifuged at 12,000×g for 15min at 4°C, and the resulting supernatant was collected for analysis. Protein concentrations were determined using a bicinchoninic acid (BCA) assay kit to ensure equal protein

loading among samples. Equal amounts of protein were mixed with 5× SDS-PAGE loading buffer (BL502A, Biosharp) and denatured by boiling at 100°C for 10min. The proteins were then separated by SDS–polyacrylamide gel electrophoresis (SDS-PAGE) and transferred onto polyvinylidene difluoride (PVDF) membranes (IPVH00010, Millipore). After blocking with 5% bovine serum albumin (BSA) for 2h at room temperature, the membranes were incubated overnight at 4°C with primary antibodies (Pan-KLA, PTM-1401RM, PTM Biolabs; H3K18la, PTM-1427RM, PTM Biolabs; PR, MA1-410, Thermo Fisher; histone H3, CPA3483, Cohesion Biosciences; β-tubulin, 10094, Proteintech) diluted according to the manufacturer's instructions. Following three washes with TBST (10min each), the membranes were incubated with HRP-conjugated secondary antibodies for 2h at room temperature. After another three TBST washes, immunoreactive signals were detected using an enhanced chemiluminescence (ECL) HRP substrate kit (K-12045-D50, Advansta) and visualized with a chemiluminescence imaging system. Densitometric analysis of immunoblot bands was performed using ImageJ software. The grey values of the target protein were first normalized against those of the corresponding internal control (β-actin or histone H3), then standardized with the mean value of the control group set as 1. All experiments were independently replicated three times (n=3 independent biological replicates).

Hematoxylin and Eosin (H&E) Staining: Whole ovaries collected from mice were fixed in 4% paraformaldehyde at room temperature for 24h. The fixed tissues were dehydrated through a graded ethanol series (70, 80, 90, 95, and 100%), with each step lasting 1h, followed by clearing in xylene and embedding in paraffin at 60°C for 3h. Serial paraffin sections (4μm thick) were obtained from a rotary microtome, floated on a 42°C water bath, mounted onto poly-L-lysine–coated slides, and dried at 60°C for 2h. Sections were deparaffinized in xylene before staining, followed by rehydration using a descending ethanol series. Slides were then stained with Harris haematoxylin solution for 5min, rinsed in running tap water for 10min for blueing, differentiated in 1% acid alcohol for 3s, and subsequently stained with 0.5% ammonia solution (blueing). The counterstain is done by 0.5% eosin solution for 1min. Lastly, sections were dehydrated by ascending ethanol series, cleared in xylene, and mounted using neutral resin. Stained sections were examined and imaged on a light microscope.

Immunohistochemical (IHC) Staining: Ovaries were harvested en bloc from mice and fixed with 4% paraformaldehyde at Room temperature overnight before being routinely embedded into paraffin wax and cut to a thickness of 4μm. Tissue sections were deparaffinized, rehydrated, and underwent antigen retrieval in pH 6.0 citrate buffer with high-pressure heat treatment (121°C, 2min) followed by natural cooling down to room temperature. Endogenous peroxidase activity was blocked through 10 minutes of incubation in 3% hydrogen peroxide solution at room temperature. Sections were blocked with 5% bovine serum albumin (BSA) for 30min and incubated with the primary antibody (including H3K18la and Pan-Kla antibodies, diluted according to the manufacturer's recommendations). After washing in PBS, sections were incubated with relevant species-matched HRP-conjugated secondary antibody at room temperature for 50min. Color development was performed using diaminobenzidine (DAB) substrate, with reaction time monitored microscopically. Nuclei were counterstained with hematoxylin for 30 seconds, differentiated in acid alcohol, and blued in water. Finally, sections were dehydrated through a graded ethanol series, cleared in xylene, and mounted with neutral resin. Positive immunostaining was visualized as yellow-brown deposits localized to antigen-expressing regions under a light microscope. For quantitative analysis, the results were presented as the ratio of positive cells to total cells.

Quantitative real-time polymerase chain reaction (qRT-PCR): Total RNA was extracted from cell samples using Trizol reagent (9109, Takara). RNA concentration and purity were assessed using a Nanodrop spectrophotometer. Subsequently, 1μg of total RNA was reverse-transcribed into cDNA using a commercial reverse transcription kit (11141ES60, YEASEN) according to the manufacturer's instructions. Quantitative real-time PCR (qPCR) was performed using the SYBR Green method (11184ES08, YEASEN). Each 20μL reaction mixture contained 10μL of 2× SYBR Premix Ex Taq, 0.4μL each of forward and reverse primers (10μM), 2μL of cDNA template, and 7.2μL of ddH_2O. Primer sequences are detailed in Tables 1, 2, 3, and 4. The amplification protocol consisted of an initial denaturation step at 95 °C for 2min, followed by 40 cycles of 95 °C for 10s and 60 °C for 30s. Tubulin (Tuba) was used as the internal reference gene, and relative gene expression levels were calculated using the $2^{\wedge(-\Delta\Delta Ct)}$ method. All samples were run in triplicate, and the entire experiment was independently repeated three times.

Chromatin Immunoprecipitation (ChIP): Chromatin immunoprecipitation (ChIP) was performed using the Pierce™ Cross-Linked Magnetic Bead Immunoprecipitation Kit (26156, Thermo Fisher Scientific) to assess the specific binding of H3K18la and PR to genomic DNA, according to the manufacturer's instructions. Briefly, cells were fixed in 1% formaldehyde for 10min at room temperature, then neutralized using glycine. Following cell lysis, chromatin was digested by micrococcal nuclease and spun down at 9000×g for 5min at 4 °C to obtain the supernatant. A 5% portion of the supernatant served as the Input control. Remaining lysate was then incubated overnight at 4 °C in the presence of a specific antibody (or control IgG). Immunocomplexes were pulled-down with Protein A/G magnetic beads, followed by elution and purification of the bound DNA. qRT-PCR analysis was performed by SYBR Green chemistry according to previously described conditions. Enrichment of target DNA fragments over Input is calculated as a percentage, following the percent input method: $\%Input = 2^{\wedge(Ct\_Input - Ct\_ChIP)} \times$ dilution factor × 100%. All samples were run in triplicate, and the experiment was independently repeated three times.

Nuclear and Cytoplasmic Protein Extraction: Nuclear and cytoplasmic protein extracts were prepared by using NE-PER™ Nuclear and Cytoplasmic Protein Extraction Kit

(78833, Thermo Fisher Scientific) following strictly the manufacturer's instruction. Briefly, after cell collection and washing with PBS, cells were resuspended in ice-cold Cytoplasmic Extraction Reagent I (CER I) supplemented with protease inhibitors and vigorously vortexed to achieve complete lysis. The lysate was incubated at ice for 10min then Cytoplasmic Extraction Reagent II (CER II). The mixture was thoroughly mixed and incubated on ice for an additional 1min. Then after centrifugation, the supernatant was collected as the cytoplasmic protein fraction, and the remainder of the pellet was resuspended in pre-chilled Nuclear Extraction Reagent (NER) containing protease inhibitors. Nuclear lysis was achieved through intermittent vortexing followed by high-speed centrifugation. Supernatants were collected to be used as nuclear protein extracts. All of these extracts were aliquoted and stored at −80 °C for future use.

Co-Immunoprecipitation (Co-IP): Immunoprecipitation (IP) was performed using Pierce™ Protein A/G Magnetic Beads (88803, Thermo Fisher Scientific) following the manufacturer's instructions. Briefly, 2×10^7 cells were harvested and washed twice using ice-cold PBS. Cells were lysed in IP lysis buffer, and lysates were centrifuged at 12,000 rpm for 15min at 4 °C to obtain the supernatant. For co-IP, An Input sample was prepared by mixing the protein lysate with 5× SDS-PAGE loading buffer and denatured at 100 °C for 10min. The rest of the lysate was incubated overnight at 4 °C with anti-PR antibody on gentle rotation. Magnetic protein A/G beads were then added into the mixtures and incubated with the antigen-antibody complexes. Beads were collected using a magnet stand, and the supernatant discarded. The immunoprecipitated complex was washed thrice with wash buffer followed by boiling in 1× SDS loading buffer (100 °C for 10min) and analyzed by Western blotting.

Statistics: All results are shown as mean±standard error of the mean (SEM), and they represent measurements taken in at least three independent experiments. Normality of data distribution was assessed using the Shapiro-Wilk test. For comparisons between only two groups, an unpaired two-tailed Student's t-test was used. For comparisons among more than two groups with one independent variable, one-way analysis of variance (ANOVA) was carried out, followed by Tukey's HSD post-hoc test to correct for multiple comparisons. Statistical analysis was done with GraphPad Prism 7 software. $P<0.05$ is considered a significant level. In all figures, *, **, and *** indicate $P<0.05$, $P<0.01$ and $P<0.001$, respectively; ns indicates not significant.

RESULTS

hCG-induced ovulation is associated with elevated lactate levels in granulosa cells: GCs depend during the follicular growth and ovulation process on glycolysis as a source of energy, given its high energetic requirement, leading to massive lactate accumulation (Wu *et al*., 2015; Sonigo *et al*., 2019). Therefore, to investigate lactate dynamics during the ovulatory time course and its role in ovulation, we used a PMSG-hCG superovulation mouse model (Fig. 1). The mice were injected with PMSG to promote follicle development and received a hCG injection after 48h to trigger ovulation, and drug treatment was applied just before hCG injection. Lactate levels in granulosa cells and ovulation rates were measured 6, 10, and 14h after hCG administration. Lactate concentrations were elevated at all three time points (Fig. 2A), whereas ovulated oocyte numbers increased only to 14h, reaching about 30 oocytes per mouse (Fig. 2B). To test whether lactate contributes to ovulation, lactate production was inhibited with the LDH inhibitor oxamate, and sodium lactate was supplied to restore lactate availability. Ovulation was assessed 14h after hCG injection. Oxamate markedly reduced lactate levels and suppressed ovulation, while lactate supplementation largely restored ovulation (Fig. 2C). Histological analysis showed increased corpora lutea after hCG stimulation. Oxamate reduced ovarian size and corpus luteum formation, and these effects were partly reversed by sodium lactate (Fig. 2D, E). Collectively, these findings demonstrate that lactate accumulation in granulosa cells is required for efficient ovulation in mice.

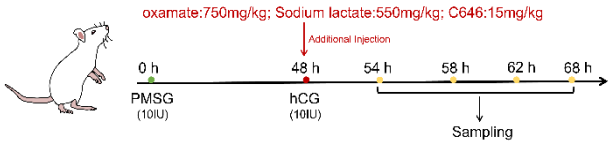

Fig 1: Schematic illustration of the in vivo experimental design. Mice were treated with 10IU PMSG to stimulate follicular growth, followed by 10IU hCG 48h later to induce ovulation. Concurrent with hCG administration, intervention groups received sodium oxamate (750mg/kg), sodium oxamate plus sodium lactate (550mg/kg), or C646 (15mg/kg) via intraperitoneal injection. Lactate levels in granulosa cells and ovulation rates were assessed at 6, 10, and 14h post-hCG, respectively, while the number of corpora lutea was determined at 20h post-hCG, with tissues collected for further analysis.

Table 1: Primer sequences used for ChIP-qPCR

Primers	Forward/Reverse	Sequences(5'-3')
Adamts1	Forward	GTGTAAGACGCCGAAACAGC
	Reverse	CAGCAGCCGAGAGATGAAGT
Adam8	Forward	CCCTGGAGCAAGGGTGTATC
	Reverse	GCTACCTTGTCAGAGTGGCT
Tnfaip6	Forward	TGCAACAAACGCCACAAACT
	Reverse	TTGCATTGGCAACCAGAACG
Pgr	Forward	AGTGGCATTCTGGGTAAGGTG
	Reverse	AGGAACAAGGAACATTGCTGAGA
Edn2	Forward	TCAGGCATGAGTTGTGCCAT
	Reverse	ATATCCCTTCGATGCGTGGG
Ptgs2	Forward	CGTCTCTCATTTGCGTGGGT
	Reverse	GGTGACTCTGTCTTTCCGCT
Runx2	Forward	CGCTCGCTTGCATTAGGAAG
	Reverse	GAGCTCGGAAAGGCTACCAG

hCG induces lactate-dependent H3K18 lactylation in granulosa cells: Because lactate is the substrate for histone lactylation (Zhang *et al*., 2019), we asked whether this modification changes after hCG injection. Western blotting of granulosa cells at 6, 10, and 14h post-hCG showed increased global lysine lactylation (Pan-Kla) at all time points, with a prominent band at about 15 kDa (Fig. 3A, C). Previous studies have reported that H3K18la is the predominant lactylation modification marker in luteinized GCs (Wu *et al*., 2024). Consistently, the present study confirmed a significant elevation of H3K18la levels during the periovulatory phase. To test whether hCG-induced H3K18la depends on lactate metabolism, we inhibited lactate production using the lactate dehydrogenase inhibitor oxamate in the presence

of hCG for 10h. The results showed that oxamate markedly reduced hCG-induced H3K18la expression, which was restored following co-treatment with sodium lactate (Fig. 3B, D). Using immunohistochemical staining, we found that hCG treatment robustly enhanced Pan-Kla and H3K18la signals in granulosa cells. However, this upregulation was suppressed by oxamate and subsequently rescued by the addition of sodium lactate. (Fig. 3E, F). These results suggest that lactate is required for hCG-induced H3K18la in granulosa cells.

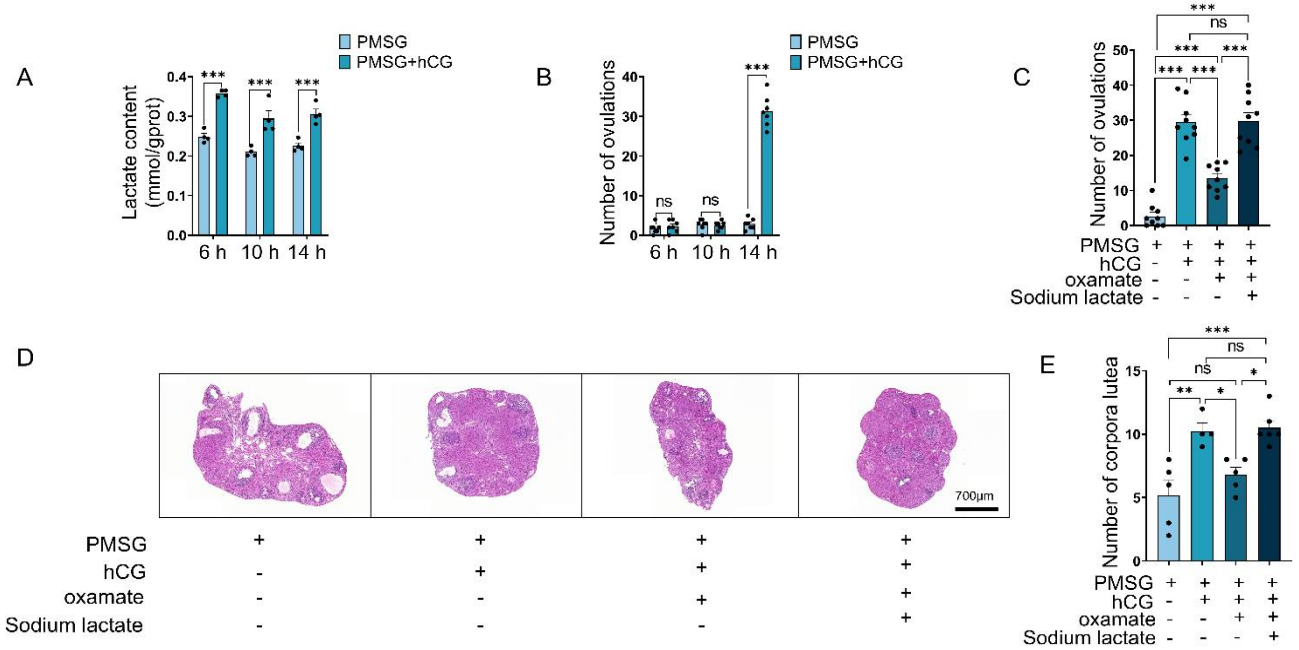

Fig 2: Lactate accumulation in granulosa cells is essential for hCG-induced ovulation. Mice were pre-treated with 10IU PMSG for 48h, followed by injection of 10IU hCG to induce ovulation. At the time of hCG injection, the respective treatment groups received either 750mg/kg oxamate, 550mg/kg sodium lactate, or an equivalent volume of saline. (A) Lactate levels in granulosa cells at 6, 10, and 14h post-hCG injection. (B) Ovulation numbers at 6, 10, and 14h post-hCG injection. Each data point represents an individual mouse (n=7 per group), the same as below. (C) Ovulation numbers at 14h after treatments that inhibited or rescued lactate levels (n=9 per group). (D) Representative H&E-stained images of ovarian tissue at 20h post-treatment, showing the morphology and quantity of corpora lutea; scale bar, 700μm. (E) Quantification of corpora lutea shown in (D). All data are presented as mean ± SEM; *P<0.05, **P<0.01, ***P<0.001.

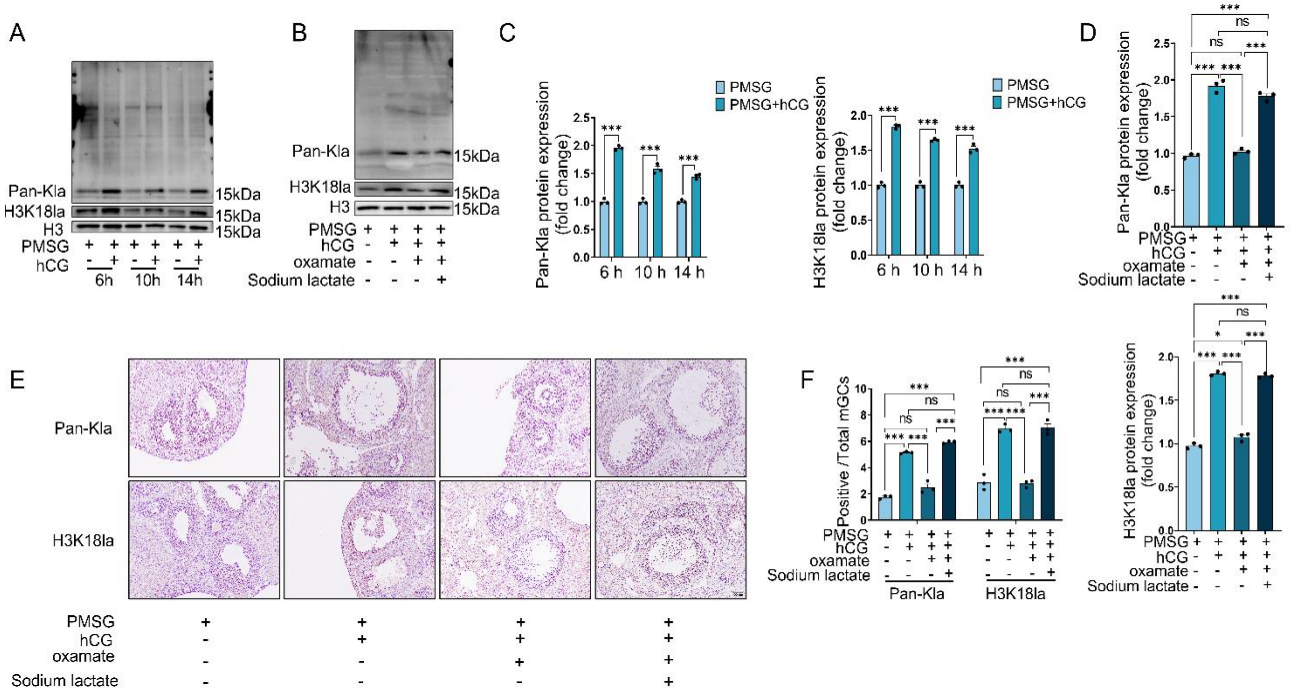

Fig. 3: hCG-driven lactate accumulation promotes H3K18 lactylation in granulosa cells. Mice were primed with 10IU PMSG for 48h, followed by 10IU hCG to trigger ovulation. At hCG administration, mice received oxamate (750mg/kg), sodium lactate (550mg/kg), or saline. (A) Representative immunoblots of Pan-Kla and H3K18la in granulosa cells at 6, 10, and 14h post-hCG. Molecular weight markers are indicated on the right of each blot, and the same below. (B) Effects of oxamate and lactate on lactylation markers at 10h post-hCG. (C, D) Densitometric analysis of lactylation levels from (A) and (B). (E) Immunohistochemical staining of Pan-Kla and H3K18la in ovarian sections at 10h post-hCG scale bar, 100μm. (F) Quantification of IHC-positive area from (E). Data are shown as mean ± SEM; *P<0.05, **P<0.01, ***P<0.001.

H3K18la is required for hCG-induced ovulation: To determine whether H3K18la contributes to hCG-induced ovulation, we treated cells with C646, an inhibitor of p300-dependent histone acylation (Dai *et al*., 2023). After 10h of co-treatment with hCG and C646, both global lysine lactylation (Pan-Kla) and H3K18la were markedly reduced (Fig. 4A-D). Immunohistochemistry confirmed a pronounced loss of H3K18la signal in granulosa cells following C646 treatment. Functionally, C646 significantly decreased the number of ovulated oocytes at 14h post-hCG administration (Fig. 4G), and H&E staining revealed a corresponding reduction in corpora lutea formation (Fig. 4E, F). This leads to the conclusion that H3K18la is essential for hCG-induced ovulation.

Table 2: Primer sequences used for qRT-PCR in primary mouse ovarian granulosa cells

Primers	Forward/Reverse	Sequences(5'-3')
Adamts1	Forward	GGGGAGACTGCTCAAGAACC
	Reverse	ACCTGTAGCGGACTCGTTTG
Adam8	Forward	AACAAGCAGCGTCTACGAG
	Reverse	TGGATTTGTCTCGGAGCCTT
Edn2	Forward	TCATCTGGGTGAACACTGCG
	Reverse	TCGATGGCAGAAGGTAGCAC
Runx2	Forward	ATGGCCAGATTCACAGTGGG
	Reverse	GGCAACGTTCCCTAACCTGA
Ptgs1	Forward	CATTGCACATCCATCCACTCC
	Reverse	ACAGGGATTGACTGGTGAGGG
Ptgs2	Forward	TTGGAGGCGAAGTGGGTTTT
	Reverse	TGGGAGGCACTTGCATTGAT
Has2	Forward	GCAGTTTTGGTGACGACAGG
	Reverse	CTTGGACCGAGCCGTGTATT
Tnfaip6	Forward	GGCTCTGCAACCGAAGAGAT
	Reverse	TTGAATCCCCATCCGTGAGC
Tuba1a	Forward	ATGTGGCAATGTGTGCTTTCAT
	Reverse	CCATAAGTGAAATGGGCAGCTT

Table 3: Primer sequences used for qRT-PCR in primary porcine ovarian granulosa cells

Primers	Forward/Reverse	Sequences(5'-3')
TNFAIP6	Forward	GTACCTCAGAGAAGCACGGT
	Reverse	ACGGCCACCTTCGTATTCAC
ADAMTS1	Forward	AGCGTCTCCTCTTTAGTGACTC
	Reverse	GCAAGACTAGCAGCGTTGTGG
RUNX2	Forward	AGCCACCTACCACAGAGCTA
	Reverse	GGATGAGGAATGCGCCCTAA
PTGS1	Forward	TTTCCGGTTTGGCATCGAGA
	Reverse	AACACCAAGCAAGACCACCA
PTGS2	Forward	TCCTGAACACCTCCGCTTTG
	Reverse	AGCCGTTCATCGTCCCATTC
TUBA1A	Forward	AAGAGTCGCGCTGTAAGAAG
	Reverse	AATGACTGTGGGTTCCAGGTC
ADAM8	Forward	CCCAGAGAGCGTGAGCTATG
	Reverse	CCACGAGGTCCCTGTTCTTC
EDN2	Forward	GTCCAGGCTGGCAAGACAT
	Reverse	TGTCCAGCAAAGCGGATTCT

H3K18la promotes PR-dependent ovulatory gene transcription: PR is a key regulator of follicular rupture, and its expression markedly upregulated by 6h after hCG stimulation. PR promotes oocyte release by activating a cascade of ovulation-associated genes (Shao *et al*., 2003). Given that histone modifications can modulate gene transcription (Bannister and Kouzarides, 2011; Stillman, 2018), we examined whether H3K18la regulates PR expression and function. Western blot analysis showed that inhibition of H3K18la with C646 significantly decreased PR protein levels (Fig. 5A, B). Consistently, qRT-PCR analysis revealed that C646 treatment markedly attenuated the hCG-induced transcriptional activation of several PR-dependent ovulation genes (Fig. 5C).

To further clarify the mechanism, we performed ChIP-qPCR to assess H3K18la enrichment at the promoter regions of *Pgr* (the gene encoding PR) and other ovulatory genes. H3K18la occupancy at the *Pgr* promoter was strongly increased 6h after hCG treatment but was abolished by C646 administration, while no enrichment was observed at other gene promoters (Fig. 5D). Furthermore, ChIP-qPCR analysis of PR binding demonstrated enhanced recruitment of PR to its target promoters following hCG stimulation, which was markedly reduced by C646 (Fig. 5E). These findings imply that H3K18la promotes ovulation by activating *Pgr* transcription and PR-dependent gene expression.

Table 4: Primer sequences used for qRT-PCR in KGN cell line

Primers	Forward/Reverse	Sequences(5'-3')
TNFAIP6	Forward	TGGAGATGAGCTTCCAGATGAC
	Reverse	GGATACAGGATCCATTGCAACAT
ADAMTS1	Forward	CTTGTGGCAGACCAGTCGAT
	Reverse	TTCACCACCACCAGGCTAAC
RUNX2	Forward	CACAAGTGCGGTGCAAACTT
	Reverse	TGACTCTGTTGGTCTCGGTG
PTGS1	Forward	TGGTTCTTGCTGTTCCTGCT
	Reverse	CTGGTGCTGGCATGGATAGT
PTGS2	Forward	ACGCTTTATGCTGAAGCCCT
	Reverse	TCCACAGCATCGATGTCACC
TUBA1A	Forward	AACCATGGTGAGAATCGGCTT
	Reverse	CAAAACATACCACCACCCTCG
ADAM8	Forward	GATGATGCTGCCTGCGATTG
	Reverse	GTAGCTCACCCTCTCTGGGT
EDN2	Forward	CCTGAACAGACAGCTCCTTACG
	Reverse	ACTGTGGAAATGTCCCAGGGC

hCG promotes PR expression and nuclear translocation via lactate to activate ovulation-related genes in porcine granulosa cells: As mentioned above, we showed that hCG regulates PR expression and function through lactate production in mice. To determine whether this mechanism is conserved in pigs, porcine granulosa cells were treated with hCG in the presence of the lactate dehydrogenase inhibitor oxamate or supplemented with sodium lactate. Consistent with murine results, hCG markedly increased PR protein levels, which were suppressed by oxamate and restored by lactate supplementation (Fig. 6A and B).

As a transcription factor, PR must translocate into the nucleus to activate target genes. Subcellular fractionation revealed that both hCG and sodium lactate significantly enhanced PR nuclear accumulation compared with oxamate treatment (Fig. 6C and D). To examine whether this process involves lactylation, PR was immunoprecipitated and probed for pan-lysine lactylation (Pan-Kla). Distinct lactylation signals were detected in PR from hCG- and lactate-treated cells but were markedly reduced by oxamate, indicating that PR undergoes lactate-dependent lactylation (Fig. 6E-G). Furthermore, inhibition of PR lactylation with the p300 inhibitor C646 reduced hCG-induced expression of downstream ovulation-related genes (Fig. 6H and I).

Taken together, these observations point to the fact that in porcine granulosa cells, lactate-dependent lactylation facilitates PR nuclear translocation and transcriptional activation of ovulatory genes, revealing a conserved metabolic–epigenetic mechanism underlying ovulation across species.

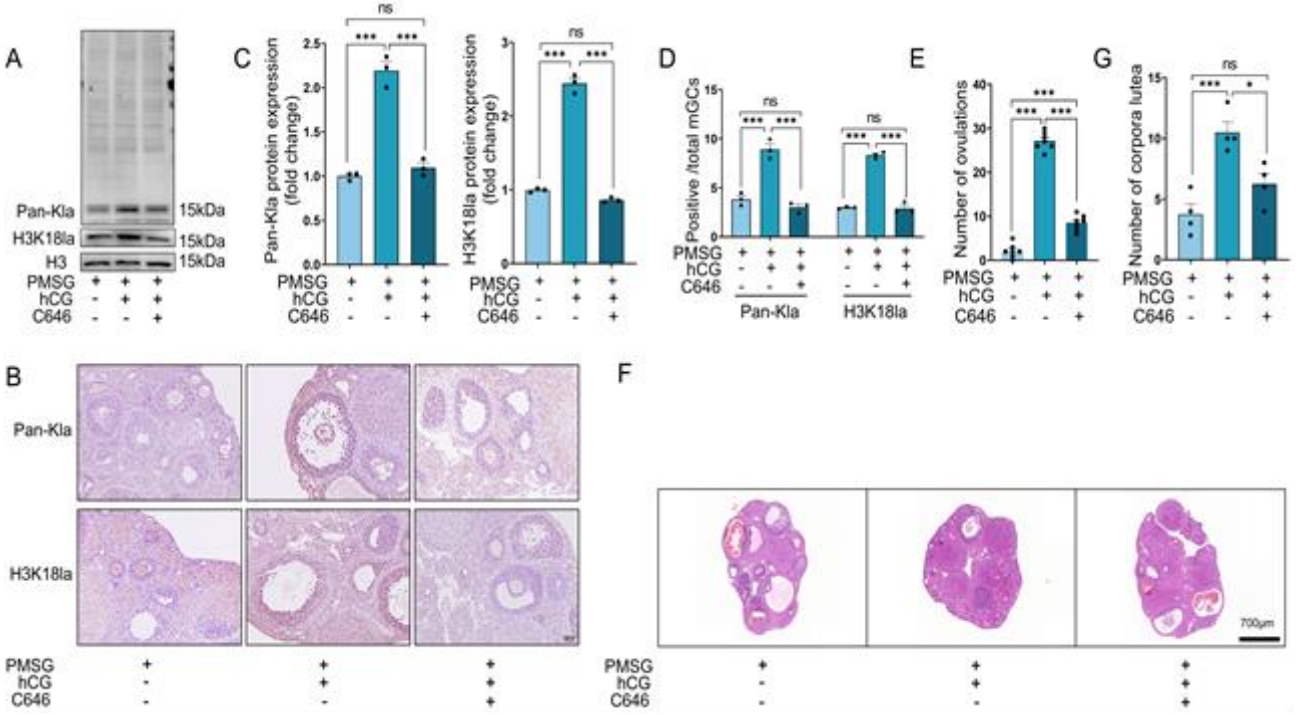

Fig. 4: Inhibition of H3K18la in granulosa cells impairs hCG-induced ovulation. Mice were pre-treated with 10IU PMSG for 48 h, followed by an injection of 10IU hCG to induce ovulation. At the time of hCG injection, treatment groups received either 15mg/kg C646 or an equal volume of saline. (A) Representative Western blots showing Pan-Kla and H3K18la levels in granulosa cells 10h after hCG injection. (B) Representative immunohistochemical staining of Pan-Kla and H3K18la in ovarian sections 10h post-hCG. scale bar, 100μm. (C) Quantification of Western blot band intensities shown in (A). (D) Quantification of positive staining areas shown in (B). (E) Ovulation numbers in each group 14h after hCG injection. (n=7 per group) (F) Representative H&E-stained ovarian sections showing corpora lutea morphology and number 20h post-treatment; scale bar, 700μm. (G) Quantification of corpora lutea shown in (F). Data are presented as mean ± SEM; *P<0.05, **P<0.01, ***P<0.001.\

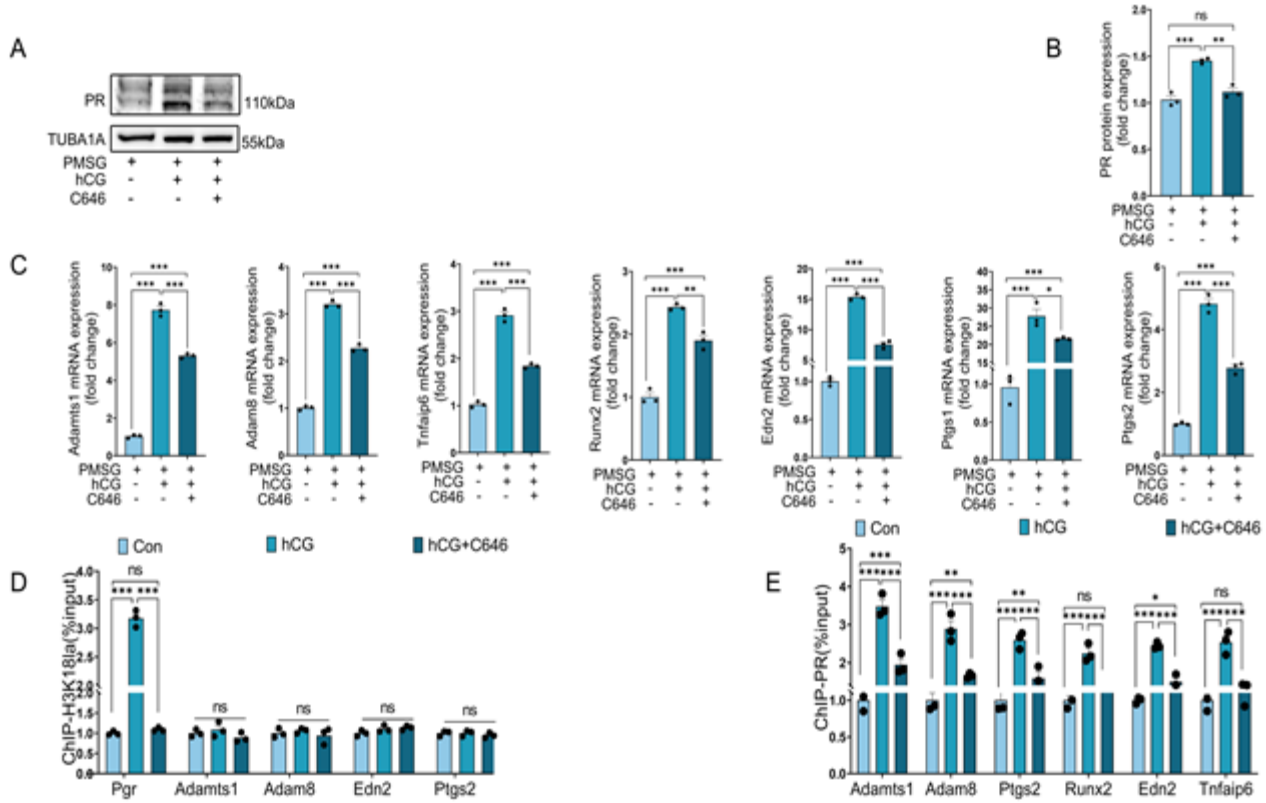

Fig. 5: Blocking H3K18la reduces PR levels and downregulates ovulatory gene expression. Mice were primed with 10IU PMSG for 48h, followed by injection of 10IU hCG to induce ovulation. At the time of hCG injection, mice received either 15mg/kg C646 or an equivalent volume of saline. (A) Representative Western blot images showing PR protein levels in granulosa cells 6h after hCG treatment. (B) Quantification of PR band intensities shown in (A). (C) Relative mRNA levels of ovulation-related genes determined by qRT-PCR 10h after hCG injection. (D) ChIP-qPCR analysis of H3K18la enrichment at the promoters of indicated genes 6h after hCG treatment. (E) ChIP-qPCR analysis of PR binding to target gene promoters 6h after hCG treatment. Data are presented as mean ± SEM; *P<0.05, **P<0.01, ***P<0.001.

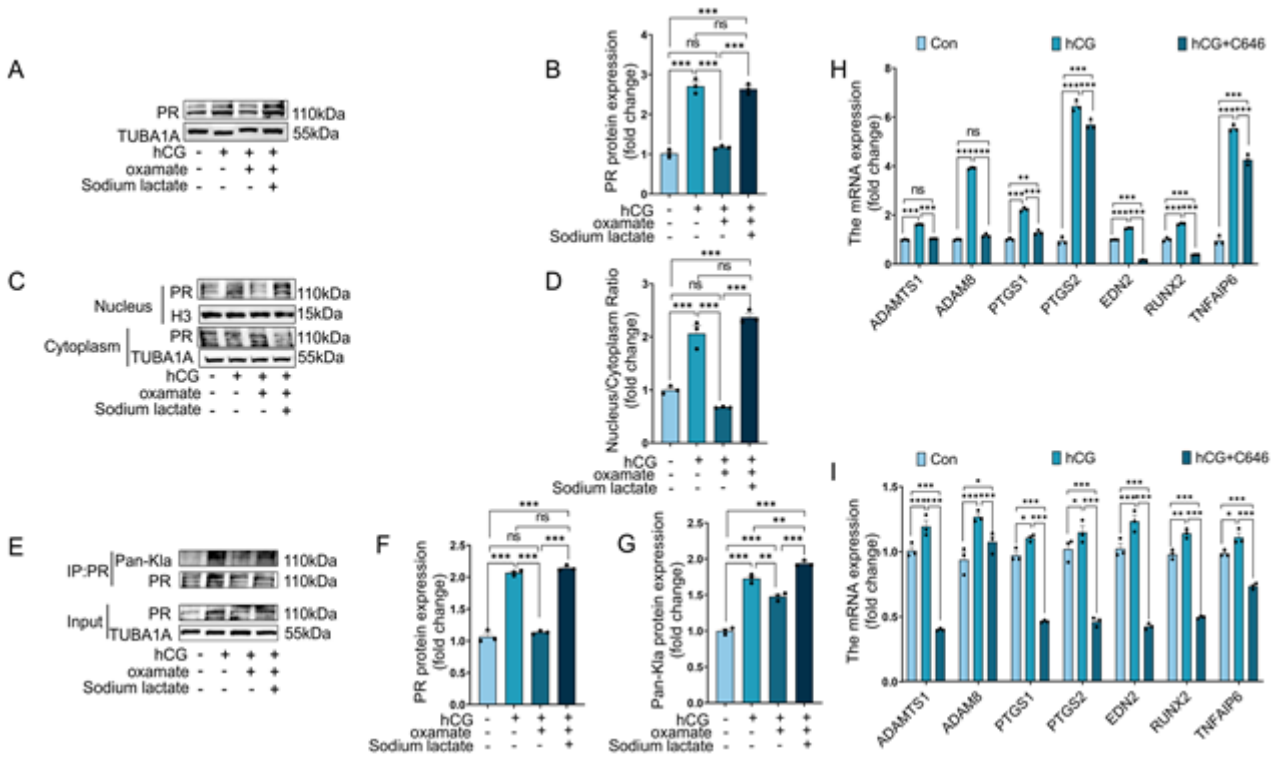

Fig. 6: Lactate regulates PR expression, nuclear translocation, and lactylation in porcine granulosa cells. Porcine granulosa cells were pretreated with 20mM oxamate for 2h prior to 10IU hCG stimulation, with or without 20mM sodium lactate supplementation. (A) Representative immunoblots of PR protein levels at 6h post-hCG. (B) Quantitative analysis of PR expression from (A). (C) Subcellular localization of PR in nuclear and cytoplasmic fractions at 6h post-hCG. β-actin and Histone H3 served as loading controls for the cytoplasmic and nuclear fractions, respectively. (D) Quantification of nuclear-to-cytoplasmic PR ratio from (C). (E) Co-immunoprecipitation analysis of PR lactylation using Pan-Kla antibody. (F) Input PR levels and (G) IP Pan-Kla levels from (E). (H-I) mRNA levels of ovulation-related genes in (H) porcine granulosa cells and (I) KGN cells at 10h post-hCG. Data represent mean ± SEM; *P<0.05, **P<0.01, ***P<0.001.

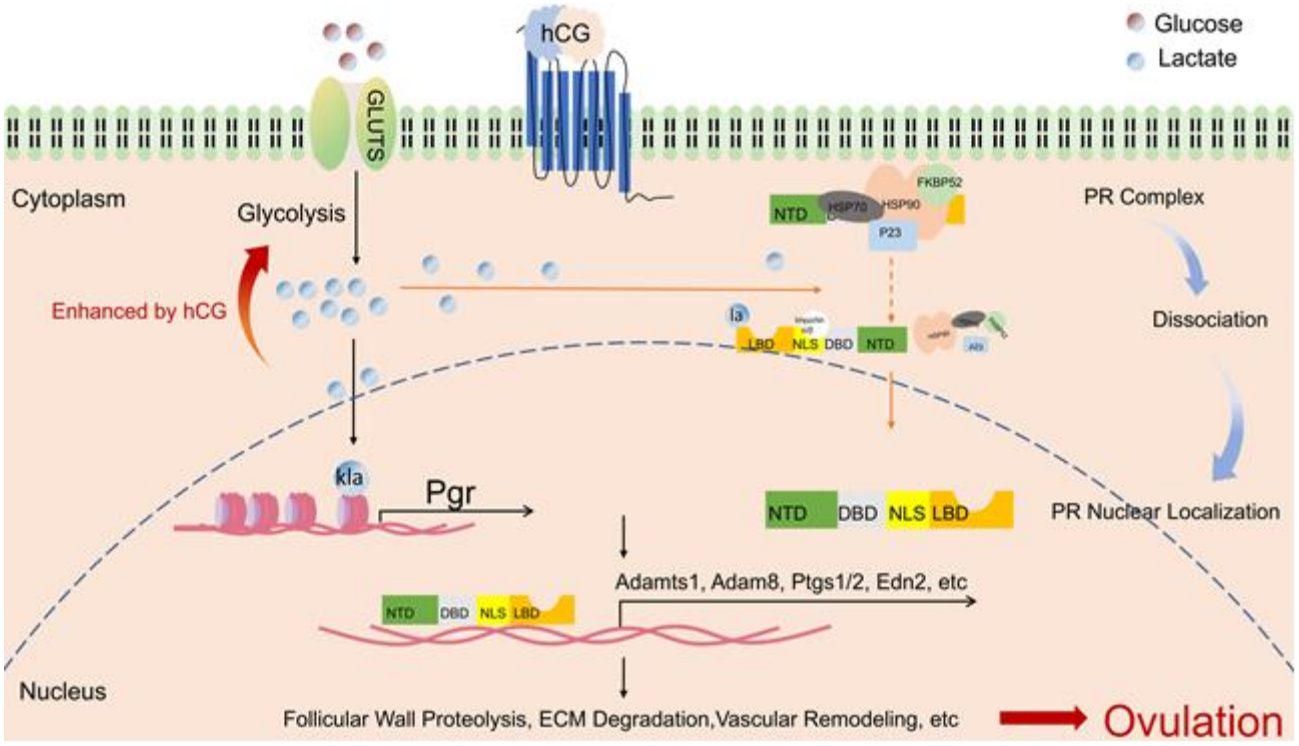

Fig. 7: Schematic diagram of H3K18 and PR lactylation mediating PR-dependent gene activation during hCG-induced ovulation. hCG stimulation elevates lactate levels in granulosa cells, triggering H3K18 lactylation (H3K18la) at the *Pgr* gene promoter and promoting PR protein lactylation. H3K18la enhances *Pgr* transcription, while PR lactylation facilitates the disassembly of its heterocomplex with co-chaperones like Hsp90. This process exposes the PR's nuclear localization signal (NLS), leading to its nuclear translocation, binding to promoters of ovulation-related genes, and the activation of a PR-dependent transcriptional program essential for follicular rupture. Abbreviation: GLUTs, Gucose Transporters; Kla, Lactylation; NTD, N-terminal Domain; DBD, DNA-Binding Domain; NLS, Nuclear Localization Signal; LBD, Ligand-Binding Domain; HSP70, Heat Shock Protein 70kDa; HSP90, Heat Shock Protein 90kDa; P23, Protein p23; FKBP52, FK506-binding protein 52kDa.

DISCUSSION

In this study, we defined a metabolic-epigenetic-transcriptional axis that couples hCG signaling to the execution of ovulation. hCG stimulation raises lactate levels in follicular granulosa cells, and this lactate both serves as a substrate for histone lactylation, notably H3K18la at the *Pgr* promoter, and promotes lactylation of the progesterone receptor (PR) protein. Based on these observations, we propose the following hypothesis. H3K18la increases *Pgr* transcription and therefore PR abundance, while PR lactylation facilitates PR nuclear accumulation and promoter recruitment. Together, they amplify PR signaling and activate a PR-dependent ovulatory transcriptional program that culminates in follicle rupture and oocyte release. (Fig. 7). Collectively, this study reveals a previously unrecognized role of lactate-driven lactylation in the regulation of ovulation.

As follicles grow, the distance between granulosa cells and follicular capillaries increases, leading to a progressively hypoxic microenvironment (Fischer *et al*., 1992). Under these low-oxygen conditions, granulosa cells rely more heavily on glycolytic metabolism, resulting in the accumulation of lactate as a major metabolic by-product (Breen *et al*., 2013; Wu *et al*., 2022). Lactate was found to facilitate early luteinization and steroidogenesis (Wu *et al*., 2024), yet its possible role in the ovulation process has been unclear. We show here that lactate accumulates in GCs during the periovulatory period and acts as more than a metabolic by-product: lactate is a signalling metabolite which regulates chromatin state via histone lactylation (Zhang *et al*., 2019; Liberti and Locasale, 2020; Malvi *et al*., 2022; Li *et al*., 2025), elevates *Pgr* transcription and PR activity, and thereby facilitates the transcriptional program required for follicle rupture. Blocking lactate production or protein lactylation impaired these responses, providing support for lactate acting as an anabolic signal during ovulation. Histone acetylation and methylation are epigenetic modifications contributing to chromatin remodeling during ovulation. Rapid remodeling of marks, including H3K4me3, after the LH surge has been linked to acute transcriptional activation in granulosa cells, and changes in histone-modifying enzyme expression have been documented during ovulation induction (Shirafuta *et al*., 2021). Histone lysine lactylation, a lactate-sensitive modification (Liberti and Locasale, 2020), rises with intracellular lactate (Zhang *et al*., 2019; Yu *et al*., 2021) and accumulates at promoters to promote transcription. In this study, we show that H3K18la functions as an upstream epigenetic regulator in the ovary by directly enriching the *Pgr* promoter and enhancing *Pgr* transcription, thereby triggering the downstream ovulatory gene program. This promoter-focused role of H3K18la mirrors its transcriptional effects reported in other systems (Galle *et al*., 2022; Tian and Zhou, 2022) and adds a novel, metabolite-linked layer to the epigenetic control of ovulation.

Importantly, our data show that PR lactylation is closely associated with enhanced PR nuclear accumulation and activation of downstream ovulatory genes. Previous studies established that PR phosphorylation and acetylation regulate its nuclear translocation and transcriptional activity (Abdel-Hafiz and Horwitz, 2014); here we identify lysine lactylation as an additional, metabolically regulated layer of PR control. Several mechanisms may underlie this effect: lactylation could modify lysines within or near nuclear localization or export motifs, thereby altering PR trafficking; it may induce conformational changes that improve PR recognition by importins or co-chaperones; or it may influence PR interactions with co-regulators or chromatin to promote nuclear retention. Crosstalk with other post-translational modifications, such as phosphorylation or acetylation (Abdel-Hafiz and Horwitz, 2014), may also contribute by competing for nearby residues or affecting the activity of enzymes such as p300 or CBP. Further clarification will require site-specific mapping by mass spectrometry and targeted mutational or biochemical assays to define how PR lactylation influences its transcriptional activity. Nevertheless, our findings provide the first evidence that lactate-dependent PR lactylation participates in regulating PR nuclear dynamics and thereby supports activation of ovulatory gene programs.

Several important limitations and avenues for future work must be acknowledged here. First, we have focussed upon the periovulatory period and do not speak to whether the lactate-lactylation axis is also operates during earlier stages of follicular development; determining whether lactylation contributes to follicle growth and acquisition of ovulatory competence will require longitudinal analyses across pre-antral and antral stages. Second, while the sensitivity to C646 and previous literature support a role of p300/CBP as mediator of lactylation, pharmacological inhibitors have off-targets effects, including on acetylation. For example, oxamate is a lactate dehydrogenase (LDH) inhibitor and could therefore impact the activity of other NADH-dependent enzymes at high concentration or under certain cell conditions. Likewise, C646 is a p300 inhibitor and therefore it could not only affect lactylation but also inhibit p300 mediated acetylation of other substrates. Genetic loss- and gain-of-function in granulosa cells along with rescue experiments will need to be performed to confirm enzyme specificity. Genetic manipulations should be incorporated into future studies, e.g., using siRNA mediated knock down of either LDHA or p300 or using CRISPR/Cas9 technology to generate gene knockout cell lines, to further specifically confirm the true role for each molecule in granulosa cell lactylation and ovulation. In addition, recent studies have implicated alternative enzymes such as AARS1 as potential lactyltransferases (Sun *et al*., 2023), and these candidates need to be tested in ovarian cells to determine which is, or are, the enzymes responsible for H3K18 and PR lactylation.

Another complexity is that lactate has pleiotropic cellular roles beyond serving as a lactyl donor. Extracellular lactate signals via the receptor HCAR1/GPR81 and can influence intracellular second-messenger pathways (Liu *et al*., 2009); intracellular lactate also alters NAD^+/NADH ratios and metabolic fluxes that affect chromatin and signaling enzymes (Haas *et al*., 2015). While our oxamate rescue and sodium lactate supplementation experiments favor a substrate-supply model for lactylation in granulosa cells, experiments that block GPR81 signaling or that profile broader metabolic changes will be necessary to distinguish receptor-mediated signaling from direct substrate-driven lactylation effects.

A key strength of this study is the integration of findings across multiple species and experimental models. The consistency observed among in vivo mouse data, primary porcine granulosa cell results, and human KGN cell line observations enhances the robustness and generalizability of our conclusions. Nevertheless, several limitations should be acknowledged. First, the KGN cell line is derived from a human granulosa cell tumor and may harbor genetic and metabolic abnormalities that do not fully recapitulate the characteristics of normal primary human granulosa cells. Second, species-specific differences in ovarian physiology and lactate metabolism may exist among mice, pigs, and humans. Therefore, while our multi-species approach increases confidence in the translational potential of our findings, future studies using primary human granulosa cells or human ovarian tissue are warranted to further validate our conclusions.

In the context of translational medicine, modern ovulation induction schemes that are based mostly on exogenous hormones, have some drawbacks including higher incidence of poor outcomes like OHSS. Findings from this study indicate that targeting lactate-H3K18la-PR axis could be used as complimentary approach for optimizing current regimes, e.g., lowering the dose of hormones. In principle it should be possible to manipulate lactate concentrations, glycolysis rates, LDH function or other enzymes involved in lactylation so as to support optimal or improved PR signal transduction and ovulatory function with reduced dependence on external hormonal agents; however, there are still a number of issues to be addressed prior to the implementation in the clinic of such approaches. Due to their widespread expression, granulosa cell-specific delivery mechanisms or highly specific lactylation modifiers would be needed before targeting these metabolicaltering enzymes or epigenetic modifiers could become clinically feasible. More preclinical research into the potential therapeutic benefits and toxicity of such compounds will be required in the future. Furthermore, since mammalian ovulation is a highly conserved process, these energy balance adaptations might be relevant to the enhancement of fertility in farm animals. In conclusion, we show that lactate-mediated lactylation plays an important role in the regulation of PR signalling during ovulation. Our data thus connect energy metabolism with gene expression upon follicle rupture, and represent a possible therapeutic target to treat ovulatory dysfunction, thereby increasing fertility.

Funding: This work was supported by the National Natural Science Foundation of China (32573216), Fundamental Research Funds for the Central Universities (KJYQ2025002), the National Key R&D Program of China (2023YFD1300502-4), the Natural Science Foundation of Jiangsu Province (BK20221512), the "Science and Technology Innovation 2030" Project (2023ZDO40710605), and the "JBGS" Project of Seed Industry Revitalization in Jiangsu Province (JBGS (2021) 026).

Authors contribution: Ming Shen conceived, designed, and supervised the study, and secured funding with Honglin Liu. Xiumei Lu performed experiments, analyzed data, and drafted the manuscript. Gang Wu, Hongmin Li, Xinyi Zhou, Junzhuo Deng, and Benlong Hua assisted with data collection, curation, and visualization. All authors reviewed and approved the final manuscript.

Declaration of Interests: The authors declare no competing interests.

REFERENCES

Abdel-Hafiz HA and Horwitz KB, 2014. Post-translational modifications of the progesterone receptors. Journal of Steroid Biochemistry and Molecular Biology 140:80-89.

Bannister AJ and Kouzarides T, 2011. Regulation of chromatin by histone modifications. Cell Research 21:381-395.

Bishop CV, Hennebold JD, Kahl CA, *et al*., 2016. Knockdown of progesterone receptor (PGR) in macaque granulosa cells disrupts ovulation and progesterone production. Biology of Reproduction 94:109.

Breen SM, Andric N, Ping T, *et al*., 2013. Ovulation involves the luteinizing hormone-dependent activation of G(q/11) in granulosa cells. Molecular Endocrinology 27:1483-1491.

Certo M, Llibre A, Lee W, *et al*., 2022. Understanding lactate sensing and signalling. Trends in Endocrinology and Metabolism 33:722-735.

Cho SE, Li W, Beard AM, *et al*., 2024. Actomyosin contraction in the follicular epithelium provides the major mechanical force for follicle rupture during Drosophila ovulation. Proceedings of the National Academy of Sciences of the United States of America 121:e2407083121.

Choi DH, Kim EK, Kim KH, *et al*., 2011. Expression pattern of endothelin system components and localization of smooth muscle cells in the human pre-ovulatory follicle. Human Reproduction 26:1171-1180.

Conti M, Hsieh M, Park JY, *et al*., 2006. Role of the epidermal growth factor network in ovarian follicles. Molecular Endocrinology 20:715-723.

Dai W, Wu G, Liu K, *et al*., 2023. Lactate promotes myogenesis via activating H3K9 lactylation-dependent up-regulation of Neu2 expression. Journal of Cachexia, Sarcopenia and Muscle 14:2851-2865.

Dinh DT, Breen J, Nicol B, *et al*., 2023. Progesterone receptor mediates ovulatory transcription through RUNX transcription factor interactions and chromatin remodelling. Nucleic Acids Research 51:5981-5996.

Fischer B, Künzel W, Kleinstein J, *et al*., 1992. Oxygen tension in follicular fluid falls with follicle maturation. European Journal of Obstetrics and Gynecology and Reproductive Biology 43:39-43.

Galle E, Wong CW, Ghosh A, *et al*., 2022. H3K18 lactylation marks tissue-specific active enhancers. Genome Biology 23:207.

Haas R, Smith J, Rocher-Ros V, *et al*., 2015. Lactate regulates metabolic and pro-inflammatory circuits in control of T cell migration and effector functions. PLoS Biology 13:e1002202.

Holesh JE, Bass AN and Lord M, 2025. Physiology, ovulation. In: StatPearls. StatPearls Publishing.

Hunzicker-Dunn M and Mayo K, 2015. Gonadotropin signaling in the ovary. In: Knobil and Neill's Physiology of Reproduction. Academic Press:895-945.

Ji S, Xi Z, Li T, *et al*., 2025. PA2G4 in CAFs promotes biochemical recurrence of prostate cancer via H3K18la. Cell Bioscience 15:152.

Johannsen ML, Poulsen LC, Mamsen LS, *et al*., 2024. The intrafollicular concentrations of biologically active cortisol in women rise abruptly shortly before ovulation and follicular rupture. Human Reproduction 39:578-585.

Kim J, Bagchi IC and Bagchi MK, 2009. Control of ovulation in mice by progesterone receptor-regulated gene networks. Molecular Human Reproduction 15:821-828.

Kim SH and Yoon JT, 2021. Morphological changes in mouse ovary due to hormonal hypersecretion and matrix metalloproteinase-2 activity. Histology and Histopathology 36:527-534.

Li M, Ma Y, Wang S, *et al*., 2025. Hypoxia promotes the in vitro proliferation of buffalo spermatogonial cells by increasing lactate and H3K18la lactylation levels. Cells 14:832.

Liberti MV and Locasale JW, 2020. Histone lactylation: a new role for glucose metabolism. Trends in Biochemical Sciences 45:179-182.

Lim M, Thompson JG and Dunning KR, 2021. Hypoxia and ovarian function: follicle development, ovulation, oocyte maturation. Reproduction 161:F33-F40.

Liu C, Wu J, Zhu J, *et al*., 2009. Lactate inhibits lipolysis in fat cells through activation of an orphan G-protein-coupled receptor, GPR81. Journal

of Biological Chemistry 284:2811-2822.

Madogwe E, Schuermann Y, Siddappa D, *et al*., 2021. Sustained ERK1/2 signaling is necessary for follicular rupture during ovulation in mice. Reproduction 161:183-193.

Malvi P, Rawat V, Gupta R, *et al*., 2022. Transcriptional, chromatin, and metabolic landscapes of LDHA inhibitor-resistant pancreatic ductal adenocarcinoma. Frontiers in Oncology 12:926437.

Migone FF, Cowan RG, Williams RM, *et al*., 2016. In vivo imaging reveals an essential role of vasoconstriction in rupture of the ovarian follicle at ovulation. Proceedings of the National Academy of Sciences of the United States of America 113:2294-2299.

Park CJ, Lin PC, Zhou S, *et al*., 2020. Progesterone receptor serves the ovary as a trigger of ovulation and a terminator of inflammation. Cell Reports 31:107496.

Park SJ, Kim TS, Kim JM, *et al*., 2015. Repeated superovulation via PMSG/hCG administration induces 2-Cys peroxiredoxins expression and overoxidation in the reproductive tracts of female mice. Molecules and Cells 38:1071-1078.

Robker RL, Russell DL, Espey LL, *et al*., 2000. Progesterone-regulated genes in the ovulation process: ADAMTS-1 and cathepsin L proteases. Proceedings of the National Academy of Sciences of the United States of America 97:4689-4694.

Schütt B, Schultze-Mosgau MH, Draeger C, *et al*., 2018. Effect of the novel selective progesterone receptor modulator vilaprisan on ovarian activity in healthy women. Journal of Clinical Pharmacology 58:228-239.

Shao R, Markström E, Friberg PA, *et al*., 2003. Expression of progesterone receptor (PR) A and B isoforms in mouse granulosa cells: stage-dependent PR-mediated regulation of apoptosis and cell proliferation. Biology of Reproduction 68:914-921.

Shirafuta Y, Tamura I, Ohkawa Y, *et al*., 2021. Integrated analysis of transcriptome and histone modifications in granulosa cells during ovulation in female mice. Endocrinology 162:bqab128.

Shynlova O, Nadeem L, Dorogin A, *et al*., 2022. The selective progesterone receptor modulator promegestone delays term parturition and prevents systemic inflammation-mediated preterm birth in mice. American Journal of Obstetrics and Gynecology 226:249.e1-249.e21.

Sirois J, Sayasith K, Brown KA, *et al*., 2004. Cyclooxygenase-2 and its role in ovulation: a 2004 account. Human Reproduction Update 10:373-385.

Sonigo C, Beau I, Grynberg M, *et al*., 2019. AMH prevents primordial ovarian follicle loss and fertility alteration in cyclophosphamide-treated mice. FASEB Journal 33:1278-1287.

Sriraman V, Eichenlaub-Ritter U, Bartsch JW, *et al*., 2008. Regulated expression of ADAM8 in the mouse ovary: evidence for a regulatory role of luteinizing hormone, progesterone receptor, and epidermal growth factor-like growth factors. Biology of Reproduction 78:1038-1048.

Stenman UH and Alfthan H, 2013. Determination of human chorionic gonadotropin. Best Practice and Research Clinical Endocrinology and Metabolism 27:783-793.

Stillman B, 2018. Histone modifications: insights into their influence on gene expression. Cell 175:6-9.

Sun L, Zhang Y, Yang B, *et al*., 2023. Lactylation of METTL16 promotes cuproptosis via m6A-modification on FDX1 mRNA in gastric cancer. Nature Communications 14:6523.

Tang Z, Xu R, Zhang Z, *et al*., 2021. HIF-1α protects granulosa cells from hypoxia-induced apoptosis during follicular development by inducing autophagy. Frontiers in Cell and Developmental Biology 9:631016.

Tian Q and Zhou LQ, 2022. Lactate activates germline and cleavage embryo genes in mouse embryonic stem cells. Cells 11:548.

Wu G, Li C, Tao J, *et al*., 2022. FSH mediates estradiol synthesis in hypoxic granulosa cells by activating glycolytic metabolism through the HIF-1α-AMPK-GLUT1 signaling pathway. Journal of Biological Chemistry 298:101830.

Wu G, Pan Y, Chen M, *et al*., 2024. Lactylation drives hCG-triggered luteinization in hypoxic granulosa cells. International Journal of Biological Macromolecules 280:135580.

Wu L, Zhang Z, Pan X, *et al*., 2015. Expression and contribution of the HIF-1α/VEGF signaling pathway to luteal development and function in pregnant rats. Molecular Medicine Reports 12:7153-7159.

Yu J, Chai P, Xie M, *et al*., 2021. Histone lactylation drives oncogenesis by facilitating m6A reader protein YTHDF2 expression in ocular melanoma. Genome Biology 22:85.

Zeng B, Knapp EM, Skaritanov E, *et al*., 2024. ETS transcription factors regulate precise matrix metalloproteinase expression and follicle rupture in Drosophila. Development 151:dev202276.

Zhang D, Tang Z, Huang H, *et al*., 2019. Metabolic regulation of gene expression by histone lactylation. Nature 574:575-580.